INVITED PAPER *Special Section on Recent Progress in Microwave and Millimeter-Wave Photonics Technology*

Standardization Activities for Radio on Fiber Transmitter within IEC TC103/WG5

Satoru KUROKAWA[†a)], **Junichiro ICHIKAWA**[††], **Tetsuya KAWANISHI**[†††], ***Members***, ***and*** **Hiroyo OGAWA**[††††], ***Fellow***

SUMMARY This paper describes the outline of recent standardization activities for Radio on Fiber (RoF) transmitter by IEC TC103/WG5. RoF transmitter consists of optical fibers, electrical to optical (E/O) converter, and optical to electrical (O/E) converter. IEC TC103/WG5 is working on standardization on measurement method of E/O and O/E devices, and technical specification of RoF transmitter. This paper overviews those standardization activities which are being developed by TC103/WG5 as well as the National Committee of WG5.
key words: *Radio on Fiber transmitter, O/E converter, E/O converter, standardization, TC103, TC103/WG5*

1. Introduction

Recent progresses in wireless communication technologies are remarkable for broadband wireless internet and mobile communication systems. RoF system is widely recognized as broadband wireless signal infrastructure to shadowing areas such as the underground, the subway stations and the inside building. Variety of RoF systems are utilized in the area of transmitting broadband wireless signal such as TV broadcasting signals, mobile phone signals and WiFi (Wireless Fidelity) signals. RoF system consists of optical fibers and microwave-photonic E/O and O/E devices. At E/O converter, optical carrier is modulated by broadband wireless signals, and the modulated optical signal is transmitted through the optical fiber. Then, the broadband wireless signals are regenerated by O/E converter. Microwave photonic devices for the E/O converter could be a $LiNbO_3$ Mach-Zehnder optical intensity modulator (MZM), an electro-absorption modulator (EAM) and a directly modulated Laser-Diode. In the case of the MZM and the EAM, high-speed modulation up to 40 GHz can be achieved for 40 Gbps digital communication systems [1]. Various types of photo diode have been used for the O/E converter. In the case of a Uni-traveling carrier photodiode (UTC-PD), 1 THz receiving bandwidth has been achieved [2], [3].

Manuscript received October 6, 2012.
Manuscript revised October 30, 2012.
[†]The author is with National Institute of Advanced Industrial Science and Technology (AIST), Tsukuba-shi, 305-8563 Japan.
[††]The author is with Sumitomo Osaka Cement CO., LTD., Funabashi-shi, 274-8601 Japan.
[†††]The author is with National Institute of Information and Communications Technology, Koganei-shi, 184-8795 Japan.
[††††]The author is with Association of Radio Industries and Businesses, Tokyo, 100-0013 Japan.
a) E-mail: satoru-kurokawa@aist.go.jp
DOI: 10.1587/transele.E96.C.138

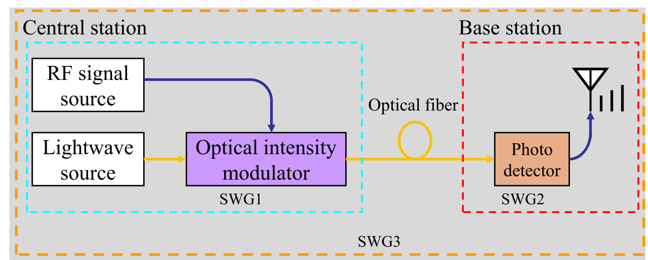

Fig. 1 Basic structure of RoF transmitter.

IEC TC103/WG5 (International Electro technical Commission Technical Committee 103 Working Group 5) has started standardization of RoF transmitter from 2005. The National Committee of TC103/WG5 consists of three sub working groups (SWGs) as follows (Fig. 1);

- SWG1: Standardization for measurement method of E/O conversion device
- SWG2: Standardization for measurement method of O/E conversion device
- SWG3: Standardization of RoF transmission system

This paper presents recent standardization activities for Radio on Fiber transmitters within IEC TC103/WG5. First, the structure of IEC standardization is explained. Next, the standardization activities for RoF transmitter in IEC TC103/WG5 as well as National Committee of WG5 are explained.

2. Structure of Standardization

2.1 Fundamental Structures of IEC Standardization

Standardizations of electronics devices and systems are mainly performed in IEC. Standardization of RoF transmitter is standardized in the IEC TC103. Table 1 shows project stages and associated documents of IEC [4]. Figure 2 illustrates the standardization procedure of IEC [4], [5]. Proposals to apply the fast-track procedure may be made some process in Fig. 2. One of the fast-track procedures is using publicly available specification that procedure needs only once voting for publication. First publication of our standardization is IEC/PAS 62593/Ed.1 [6]. Currently, we have four approved new work items that were developed during the expert meetings with consideration of experts'

Table 1 Project stages and associated documents [4].

Project stage	Associated document	
	Name	Abbreviation
Preliminary stage	Preliminary work item	PWI
Proposal stage	New work item proposal[1)]	NP
Preparatory stage	Working draft(s) [1)]	WD
Committee stage	Committee draft(s) [1)]	CD
Enquiry stage	Enquiry draft [2)]	ISO/DIS IEC/CDV
Approval stage	Final draft International Standard [3)]	FDIS
Publication stage	International Standard	ISO, IEC or ISO/IEC

1) These stages may be omitted, as described in Annex F [4].
2) Draft International Standard in ISO, committee draft for vote in IEC.
3) May be omitted

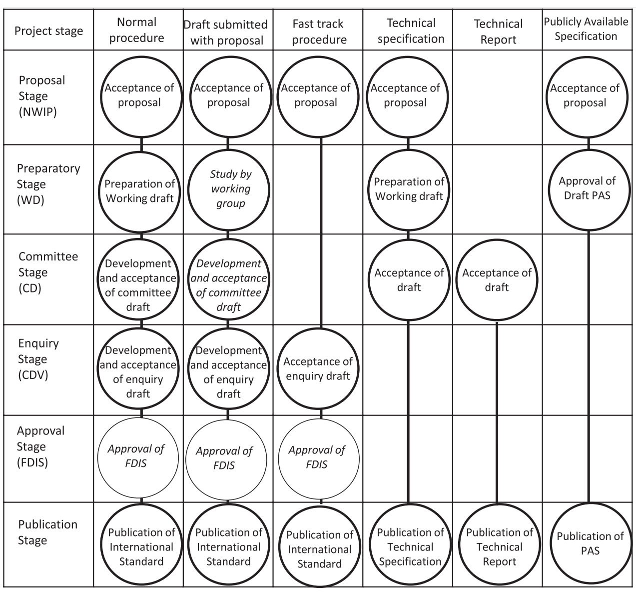

Fig. 2 Standardization procedures of IEC [4].

comments [7]–[10]. IEC TC103/WG5 decided that the documents should be promoted from the Working Draft (WD) stage to the Committee Draft (CD) stage. The documents are currently approaching the final committee draft phase of the IEC approval process.

After this section, an overview of these four documents is described.

2.2 Reference Model and Related Technical Committees of TC103

Related topics of optical devices for digital communication systems are treated in TC86. The Hybrid Fiber-Coax (HFC) transport network (HFC) is treated in TC100/TA5. Figure 3 shows the reference model of each TC. Electrical passive devices for high frequency (RF and microwave) range are treated in TC46. However, E/O and O/E devices are mainly used RoF transmitters. For these reason, these devices and RoF transmitter system is treated in TC103/WG5.

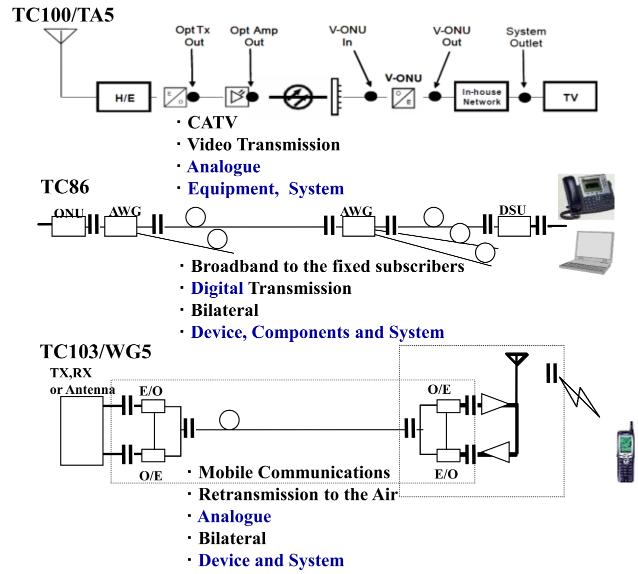

Fig. 3 Reference model of photonic standardization technical committee related to TC103.

3. Standardization for Measurement Method of E/O Conversion Device

SWG1 of TC103/WG5 is in charge of standardizing the measurement method for E/O conversion devices. Our standardized methods are described in Table 2. Method A, using electrical oscilloscope, is used for the frequency range less than 30 GHz. Method B, C and D, using optical spectrum analyzer, are used for the frequency range more than 10 GHz. [Accuracy of half-wavelength voltage] and [Accuracy of chirp parameter] in Table 1, '+++' indicates the most accurate method in method A, B, C and D. [NA] in its column indicates that the method cannot measure the chirp parameter. [Requires No. of Spectra] indicates the required number of optical frequencies for evaluating the half-wavelength voltage and the chirp parameter. [NA] indicates that the method doesn't use optical a frequency for need evaluating the half-wavelength voltage. Method A has been already published as an IEC/Publicly Available Specification (PAS) titled "Measurement Method of a Half-Wavelength Voltage for Mach-Zehnder Optical Modulator in Wireless Communication and Broadcasting Systems" [6] Our new work item proposal (NWIP) of the International Standard also has been accepted and the project was registered as IEC 62801 Ed. 1.0 [7]. Now the revised draft is ready to be circulated as CDV. CDV is the last possible moment at which changes can still be made to the content of an International Standard. Method B, C and D are the method for measuring the half-wavelength voltage and chirp parameter of MZM more than 10 GHz [11]–[13] that has been also approved as a NWIP [9], [12]. The project was registered as IEC 62802 Ed. 1.0 "Measurement Method of a Half-Wavelength Voltage and a Chirp Parameter for Mach-Zehnder Optical Modulator in High-Frequency Ra-

Table 2 Comparison between method A, B, C and D.

Method	Bias condition	Accuracy of half-wavelength voltage	Accuracy of chirp parameter	Required No. of Spectra	Required RF power
Method A[6][7] < 30GHz	Fixed bias point	+++	NA	NA	Large
Method B [9] > 10GHz	Fixed bias point	++	++	1	Middle
Method C [9] > 10GHz	Swept bias	+++	+++	1	Middle
Method D [9] > 10GHz	Minimum /Maximum transmission bias	++	+	2	Small

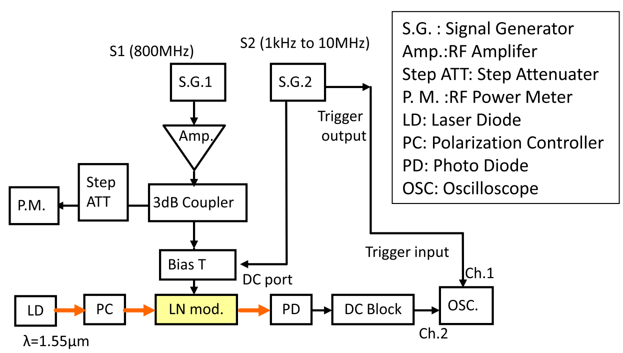

Fig. 4 Driving voltage measurement setup.

dio on Fiber (RoF) Systems" [9]. The revised draft will be circulated shortly to National Committees as CD for comment. This stage is the principal stage at which comments from member countries are taken into consideration, with a view to reaching consensus on the technical content.

3.1 Measurement Principle of Half-Wavelength Voltage for Low Frequency Range [6], [7]

The method for measuring the half-wavelength voltage of $LiNbO_3$ Mach-Zehnder optical intensity modulator, using standard electrical oscilloscope, is described here. Figure 4 shows the driving voltage, such as $V\pi$, measurement setup.

The optical output power of MZM is given by:

$$I = \frac{I_0}{2}\left[1 + \cos\left(\Phi_1 + \Phi_2\right)\right] \tag{1}$$

$$\Phi_1 = \frac{\pi V_{\rm pp}}{2V_\pi}\sin\left(2\pi f t\right) \tag{2}$$

$$\Phi_2 = \text{const.} \tag{3}$$

where Φ_1 and Φ_2 are the phase changes caused by the high-frequency RF signal (SG1) and low frequency RF signal (SG2) that due to the bias voltage, respectively. $V\pi$ is the half-wavelength voltage at the RF signal frequency f, $V_{\rm pp}$ is the peak-to-peak voltage amplitude of the high-frequency wave, and I_0 is the maximum optical output power. The time average power of I, I' is calculated by,

$$I' = f\int_0^{1/f}\frac{I_0}{2}\left[1 + \cos\left(\Phi_1 + \Phi_2\right)\right]dt$$

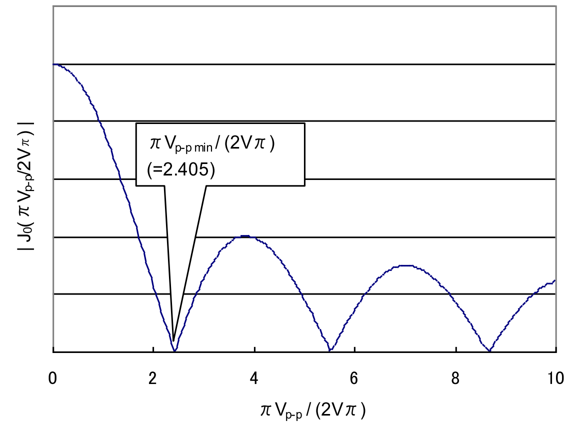

Fig. 5 Zero-order Bessel function.

$$= f\int_0^{1/f}\frac{I_0}{2}\left[1+\cos\Phi_1\cos\Phi_2-\sin\Phi_1\sin\Phi_2\right]dt \tag{4}$$

Then, we get Eq. (5)

$$\begin{aligned}
I' &= f\int_0^{1/f}\frac{I_0}{2}\left[1+\cos\left\{\frac{\pi V_{\rm pp}}{2V_\pi}\sin\left(2\pi f t\right)\right\}\cos\Phi_2\right.\\
&\quad\left.-\sin\left\{\frac{\pi V_{\rm pp}}{2V_\pi}\sin\left(2\pi f t\right)\right\}\sin\Phi_2\right]dt\\
&= f\int_0^{1/f}\frac{I_0}{2}\left[1+\sum_{n=0}^{\infty}\varepsilon_n\cos\left(2n\cdot 2\pi f t\right)J_{2n}\left\{\frac{\pi V_{\rm pp}}{2V_\pi}\right\}\cos\Phi_2\right.\\
&\quad\left.-\sum_{n=0}^{\infty}2\sin\left\{\left(2n+1\right)2\pi f t\right\}J_{2n+1}\left\{\frac{\pi V_{\rm pp}}{2V_\pi}\right\}\sin\Phi_2\right]dt\\
&= \frac{I_0}{2}\left[1+J_0\left(\frac{\pi V_{\rm pp}}{2V_\pi}\right)\cos\Phi_2\right]
\end{aligned} \tag{5}$$

Where,

$$\varepsilon_n = \begin{cases} 1\cdots n = 0 \\ 2\cdots n \neq 0 \end{cases}$$

When the input RF signal is tuned so that the relation

$$\pi\cdot V_{\rm pp}/(2V\pi) = 2.405$$

can be satisfied, the zero-order Bessel term in Eq. (5) becomes zero and the time average of the optical output power becomes constant. As shown in Fig. 5, there are many voltage amplitudes at which the AC component of I' goes down to zero; $V_{\rm pp\,min}$ denotes the lowest one.

Figure 6 shows the measurement process of using a synchronizing oscilloscope. In order to easily find the state where the optical output is constant, a low frequency signal for monitoring (SG2) is superimposed on the RF signal. By adjusting the RF voltage amplitude of the high-frequency signal (SG1), the status can be observed where the monitored signal (SG2) amplitude shows the minimum value. At this status, the waveform of the monitor signal is observed as a flat line (Fig. 6(b)) on the oscilloscope screen. $V\pi$ at the frequency of SG1 can be calculated from the measured result of P_{S1} dBm using the following relation:

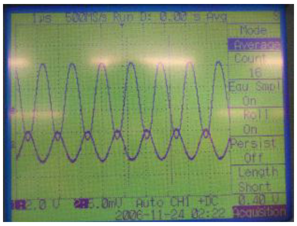

(a)The optical sugnals is modulated in opposite phase with S2 element.

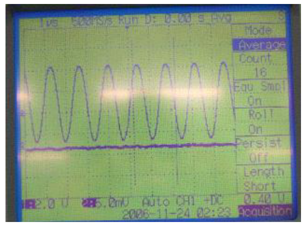

(b)The amplitude of optical signal is almost zero

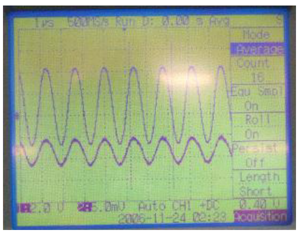

(c)The optical sugnal is modulated in phase with S2 element.

Fig. 6 $V\pi$ voltage measurement procedure.

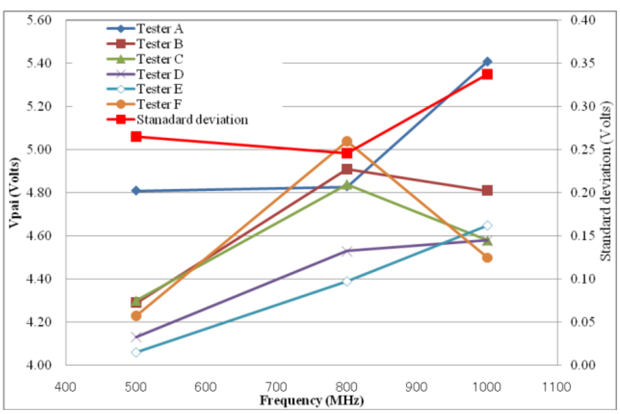

Fig. 7 Measured $V\pi$ voltage and its standard deviations of a traveling wave electrode type MZM.

$$V_\pi = \frac{\pi \cdot 20\left(10^{((P_{S1}/10)-3)}\right)^{1/2}}{2 \times 2.405} \tag{6}$$

In the case of the characteristic impedance of the electrode of the LN modulator $Z_0 = 50\,\Omega$, $V\pi$ can be estimate by:

$$V_\pi = \frac{\pi \cdot V_{\text{pp min}}}{2 \times 2.405} \tag{7}$$

3.2 Round Robin Test Results

International round robin (RR) tests were performed from 2007 to 2008. Singapore, France, Portugal, China and Japan joined this international RR test. Figure 7 shows the measured $V\pi$ voltage and standard deviations of a traveling wave electrode type MZM. The standard deviation of this measurement is less than 6.4%. Figure 8 shows the measured $V\pi$ voltage and standard deviations of a resonant electrode type MZM. The standard deviation of this measurement is less than 5.0%. These measurement results show good agreement using our standardization procedure.

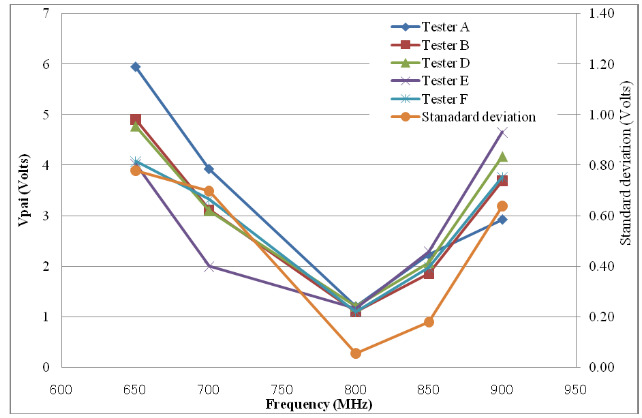

Fig. 8 Measured $V\pi$ voltage and its standard deviations of resonant electrode type MZM.

3.3 Measurement Principle of Half wave Voltage and Chirp Parameter for High Frequency Range [9], [11]–[13]

The method for measuring the half-wavelength voltage of the MZM (Method B, C and D), using optical spectrum analyzer (OSA), is described here.

When a single-tone RF signal is applied to the modulator, the optical output would have sideband components whose frequency separation is equal to the frequency of the single-tone RF signal. The induced optical phases in a MZ modulator can be calculated from the intensities of the optical sideband components measured by the OSA. When the input RF power or voltage is also measured at this condition, the half-wavelength voltage ($V\pi$) can be determined. This measurement can be achieved through a wide frequency range more than 10 GHz, which depends on the minimum resolution of OSA.

Optical output of an MZM is given by,

$$\begin{aligned} E &= \frac{E_i e^{j\omega_0 t}}{2}\left\{\exp j\left[A_1 \sin\omega_m t + \phi_{B1}\right] + \exp j\left[A_2 \sin\omega_m t + \phi_{B2}\right]\right\} \\ &= \frac{E_i e^{j\omega_0 t}}{2}\left\{e^{j\phi_{B1}}\sum_{n=-\infty}^{\infty} J_n(A_1) e^{jn\omega_m t} + e^{j\phi_{B2}}\sum_{n=-\infty}^{\infty} J_n(A_2) e^{jn\omega_m t}\right\} \\ &= \frac{E_i e^{j\omega_0 t} e^{j\phi_{\overline{B}}}}{2}\left\{e^{-j\phi_B/2}\sum_{n=-\infty}^{\infty} J_n(A_1) e^{jn\omega_m t} + e^{j\phi_B/2}\sum_{n=-\infty}^{\infty} J_n(A_2) e^{jn\omega_m t}\right\} \end{aligned} \tag{8}$$

$$\phi_{\overline{B}} = \frac{\phi_{B1} + \phi_{B2}}{2}, \quad \phi_B = -\phi_{B1} + \phi_{B2} \tag{9}$$

where ϕ_{B1} and ϕ_{B2} are the optical phase delays at two arms in the Mach-Zehnder interferometer in the modulator. The phase difference ϕ_B can be controlled by dc bias voltage applied on the electrode of the modulator. $E_i e^{i\omega_0 t}$ is the electric field of the input lightwave, where ω_0 is the angular frequency of the input lightwave and ω_m is that of the RF signal. A_1 and A_2 are the optical phase retardation due to the RF signal fed to the electrode in the modulator. J_n is the first kind Bessel's function. Intensities of sideband components, which correspond to the n-th order terms in Eq. (9), can be measured by using an OSA. Thus, we can get nonlinear simultaneous equations for A_1 and A_2. The half-wavelength voltage V_π was derived from A_1 and A_2 by using

$$V\pi = \frac{\pi V_{pp}}{2(A_1 - A_2)}, \tag{10}$$

If we consider the case of a small amplitude modulation where A_1 and $A_2 < 1$, the chirp parameter, the ratio of the amplitude modulation and the phase modulation, can be described by

$$\alpha_0 = \frac{A_1 + A_2}{A_1 - A_2}, \tag{11}$$

where the dc bias is $\phi_B = \pi/2$, which corresponds to an optimal condition for small amplitude modulation. A_1 and A_2 have opposite polarity in properly designed MZMs using push-pull configuration which provides effective intensity modulation. If the modulator has a symmetric structure with respect to the optical waveguide, A_1 equals $-A_2$, so that α_0 equals 0, which corresponds to a zero-chirp modulator. Assuming that nonlinear optical effects except the Pockels effect are negligible, the ratio between A_1 and A_2 does not depend on the intensity of the electric signal. Thus, α_0 is also an intrinsic parameter of the modulator. There are various options in selection of the simultaneous equations.

3.3.1 Measurement Principle of Half-Wavelength Voltage and Chirp Parameter with Fixed Dc-Bias Condition (Method B) [12]

The ratio between the n-th and (n+1)-th order sideband intensities in the optical spectrum is expressed by

$$\begin{aligned} R_n &= \frac{\left|J_n(A_1) + J_n(A_2)e^{j\phi_B}\right|^2}{\left|J_{n+1}(A_1) + J_{n+1}(A_2)e^{j\phi_B}\right|^2} \\ &= \frac{\{J_n(A_1)\}^2 + \{J_n(A_2)\}^2 + 2J_n(A_1)J_n(A_2)\cos\phi_B}{\{J_{n+1}(A_1)\}^2 + \{J_{n+1}(A_2)\}^2 + 2J_{n+1}(A_1)J_{n+1}(A_2)\cos\phi_B} \end{aligned} \tag{12}$$

If the electrode is not dc-coupled, the phase difference ϕ_B cannot be controlled by the bias voltage. Thus, we need to solve simultaneous equations for ϕ_B, A_1 and A_2. For example, by using three equations, R_0, R_1, and R_2, we can obtain ϕ_B, A_1 and A_2. When ϕ_B can be precisely controlled, A_1 and A_2 can be determined from two of R_n' s. The number of equations is equal to that of unknown variables, but these equations are transcendental. Thus, several solutions may be derived, and some of them may have no physical meaning. Actual solutions can be obtained by using more equations than the number of unknown variables.

3.3.2 Measurement Principle of Half-Wavelength Voltage and Chirp Parameter Using Dc-Bias Sweep (Method C) [12]

Factor $\cos\phi_B$ in Eq. (12) shows the connection between the optical spectrum and the dc-bias voltage. ϕ_B depends on the environmental conditions, which is known as dc-drift. Because the half-wavelength voltage $V\pi$ does not change much, the effect of dc-drift can be eliminated by sweeping the dc-bias voltage across two times $V\pi$ for dc, which corresponds to a period of $\cos\phi_B$ The ratio of the optical sideband intensities is expressed by

$$R_n = \frac{\{J_n(A_1)\}^2 + \{J_n(A_2)\}^2}{\{J_{n+1}(A_1)\}^2 + \{J_{n+1}(A_2)\}^2} \tag{13}$$

and does not depends on the dc-bias voltage, so A_1 and A_2 can be precisely determined.

3.3.3 Measurement Principle of Half-Wavelength Voltage and Chirp Parameter Using Minimum Transmission Bias and Maximum Transmission Bias (Method D) [12]

If the ϕ_B can be precisely controlled, A_1 and A_2 can be obtained from the 0-th and 1st order sideband components, where two types of dc-bias conditions are used. The intensity of the n-th order sideband can be expressed by,

$$\begin{aligned} P_n &= E_i^2 \frac{\left|J_n(A_1) + J_n(A_2)e^{j\phi_B}\right|^2}{4} \\ &= E_i^2 \frac{\{J_n(A_1)\}^2 + \{J_n(A_2)\}^2 + 2J_n(A_1)J_n(A_2)\cos\phi_B}{4} \end{aligned} \tag{14}$$

When no RF signal is applied to the modulator, A_1 and A_2 are equal to zero. The optical power is given by

$$P_0' = E_i^2 \frac{1 + \cos\phi_B}{2}, \tag{15}$$

P_0' depends on the dc-bias and E_i^2 shows the peak power of the optical output without RF signal input. We use two dc-bias points, the maximum transmission bias $\phi_B = 0$ ($P_0' = E_i^2$), and the minimum transmission bias $\phi_B = \pi$ ($P_0' = 0$). At the maximum transmission bias P_0 has the maximum (P_{0a}), while P_1 has the minimum. At the minimum transmission bias P_1 has the maximum (P_{1b}), while P_0 has the minimum. Thus, we can accurately measure P_0 at the maximum transmission bias, and P_0 at the minimum transmission bias, because the other spectral components are much smaller than the desired component. P_{0a} and P_{1b} are normalized by E_i^2, and expressed by

$$\frac{P_{0a}}{E_i^2} = \frac{\{J_0(A_1)\}^2 + \{J_0(A_2)\}^2 + 2J_0(A_1)J_0(A_2)\cos\phi_B}{4} \tag{16}$$

$$\frac{P_{1b}}{E_i^2} = \frac{\{J_1(A_1)\}^2 + \{J_1(A_2)\}^2 - 2J_1(A_1)J_1(A_2)\cos\phi_B}{4}. \tag{17}$$

P_{0a}/E_i^2 and P_{1b}/E_i^2 can be measured by an OSA or an optical power meter. A_1 and A_2 are determined from Eqs. (16) and (17).

4. Standardization for Measurement Method of O/E Conversion Device [10], [14]–[16]

SWG2 of TC103/WG5 is in charge of standardizing the

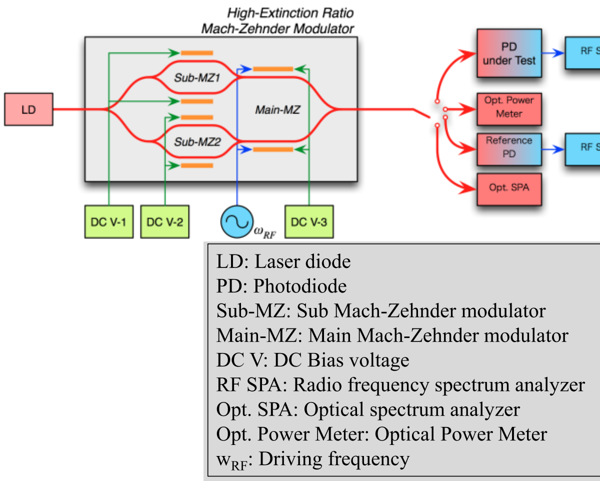

Fig. 9 Measurement setup for O/E devices.

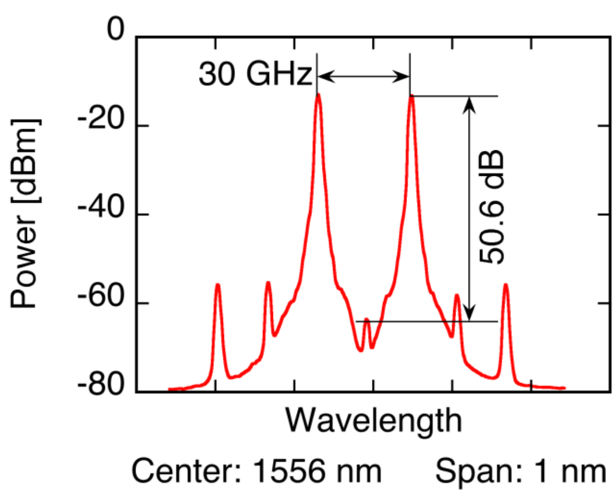

Fig. 10 A generated two-tone lightwave using nested MZM of Fig. 9 with carrier suppression bias voltage condition.

measurement method for O/E conversion devices. The proposed method is described here. Our NP of the measurement method was accepted and registered as IEC 62803 Ed. 1.0 (NP) [10].

Our method is based on the heterodyne principle. The method utilizes a MZM for generating two-tone lightwaves as stimulus signals, to provide simpler and easier methods than the conventional method utilizing a complex two-laser system phase-locked with each other. Figure 9 shows the measurement setup of our method. Figure 10 shows a generated two-tone lightwave using nested MZM of Fig. 9. A two-tone lightwave illuminates the DUT (Device Under Test) as a stimulus signal. The two-tone stimulus lightwave is generated by using an MZM at null bias or at full bias with an optical band rejection filter. The average powers of the input two-tone lightwave and that of the output monotone RF signal are measured, and the conversion efficiency at the frequency is calculated from them. By changing the frequency difference between the two tones, the frequency response of O/E conversion efficiency of the DUT is obtained.

An MZM optical output modulated by a monotone RF signal can be expressed by

$$\begin{aligned} E_{opt} &= \sum_{n=-\infty}^{\infty} E_n\, e^{i(\omega_n t+\phi_n)}, \\ P_{opt} &= \sum_{n=-\infty}^{\infty} P_n, \\ P_n &= |E_n|^2, \\ \omega_{n+1} - \omega_n &= \omega_{RF} \end{aligned} \tag{18}$$

where P_{opt} is the total average power, and ω_{RF} is the angular frequency of modulating RF signal that corresponds to the angular frequency difference between adjacent optical tones. As an example, two-tone signal generation by an MZM with null-bias is described in this section. When

$$\begin{aligned} &|E_{-1}| = |E_{+1}| \gg |E_n|\,(n \neq -1, +1), \\ &P_{opt} \cong |E_{-1}|^2 + |E_{+1}|^2 = 2\,|E_{-1}|^2 \end{aligned} \tag{19}$$

an ideal well-balanced optical two-tone consisting of $P_{\pm 1}$ can be generated, where the following conditions should be satisfied.

1. Suppression of optical carrier and higher order sidebands should be large enough.
2. Frequency difference between the two desired components should be stable.
3. Polarizations of the two spectral components should be well aligned.
4. Power difference of the two spectral components should be small enough.

The instantaneous optical power P_{opt} illuminating the PD is calculated as

$$\begin{aligned} P_{opt} = &\Big| E_{-1} e^{i(\omega_{-1}t+\phi_{-1})} + E_{+1} e^{i(\omega_{+1}t+\phi_{+1})} \\ &+ \sum_{n=-\infty}^{\infty} E_n e^{i(\omega_n t+\phi_n)} \Big|^2 (n \neq -1, +1) \\ \cong\ & P_{opt} + P_{opt} \cdot \cos(2\omega_{RF} t + \phi) \end{aligned} \tag{20}$$

where $\phi = \phi_{-1} - \phi_{+1}$, and $|E_n|$ $(n \neq -1, +1)$ related terms are neglected from the last equation. The PD under test outputs a DC and an RF photocurrent as a response. The RF photocurrent i_{RF} is expressed as

$$i_{RF} = \sqrt{\kappa} \cdot P_{opt} \cdot \cos(2\omega_{RF} t + \phi) = I_{RF} \cos(2\omega_{RF} t + \phi) \tag{21}$$

where κ is the frequency response of the PD under test at $2\omega_{RF}$, and I_{RF} is the peak photocurrent. The average RF power P_{RF} driving a load Z_L of $50\,\Omega$ is expressed as

$$P_{RF} = \frac{I_{RF}}{\sqrt{2}} \cdot \frac{I_{RF}}{\sqrt{2}} Z_L = 25 I_{RF}^2 \tag{22}$$

From Eqs. (21) and (22), the frequency response κ of the PD is calculated as

$$\kappa = \frac{I_{RF}^2}{P_{opt}^2} = \frac{P_{RF}}{25 P_{opt}^2} \tag{23}$$

Note that κ can be calculated only from the input optical and

Table 3 O/E devices for trial measurement.

	PD1	PD2
Manufacturer	NTT electronics	u²t Photonics
Model No.	KEPD2562KCG	XPDV2150R
DC responsively	0.53 A/W	0.65 A/W typ.
3 dB bandwidth	20 GHz	50 GHz

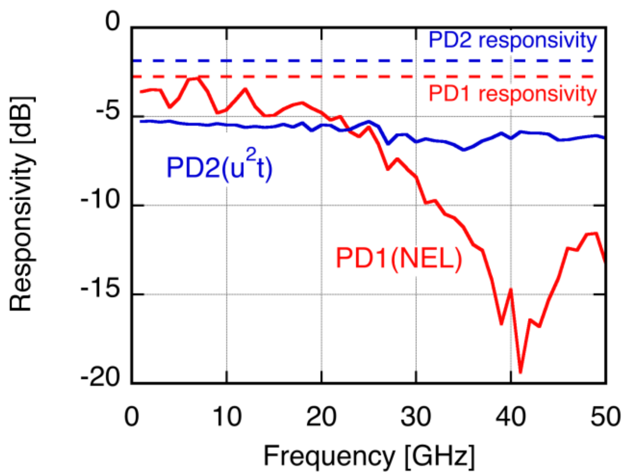

Fig. 11 Measurement results of O/E devices.

the output RF average powers of the PD under test, which are traceable to the national standards with relatively short traceability chain. In this method, κ does not depend on frequency response of the MZM used for two-tone generation.

As for the PDs under trial measurement, we use two PDs with different 3 dB bandwidths listed in Table 3. Figure 11 shows the results of the trial measurement from 1 GHz to 50 GHz frequency range. Their performance difference in 3 dB bandwidth is clearly demonstrated.

5. Technical Specification of RoF Transmitter to Conform Spectral Emission Standards [8]

SWG3 of TC103/WG5 is in charge of standardizing RoF systems. The first NP concerning the system is the technical specification (TS) of RoF transmitter which was accepted and registers as IEC 62800 Ed. 1.0 "Radio on Fiber System conforming to different Spectral Emission Standard" [8]. Our proposed TS is described here.

This Technical Specification specifies the parameters of the Radio on Fiber (RoF) system to conform to different spectral emission standards of mobile communication system and digital terrestrial television broadcasting (DTTB) defined by ITU-R (International Telecommunication Union-Radio communication Sector) Recommendations. Figure 12 shows a reference model of RoF transmitter. The reference model consists of E/O and O/E modules that are connected to a transceiver or antenna, optical networks, and E/O and O/E modules that are connected to a transceiver or antenna

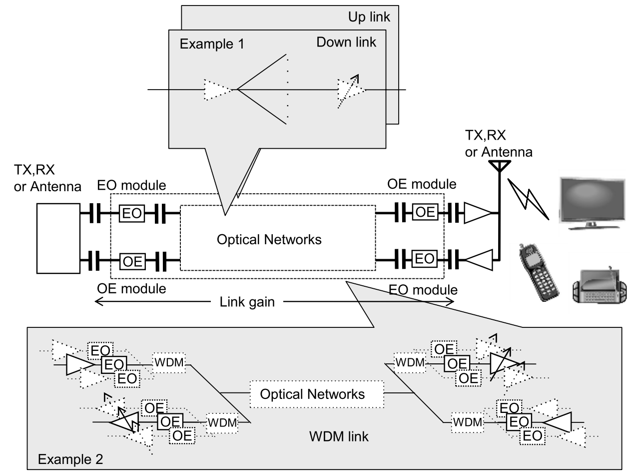

Fig. 12 Reference model of RoF transmitter.

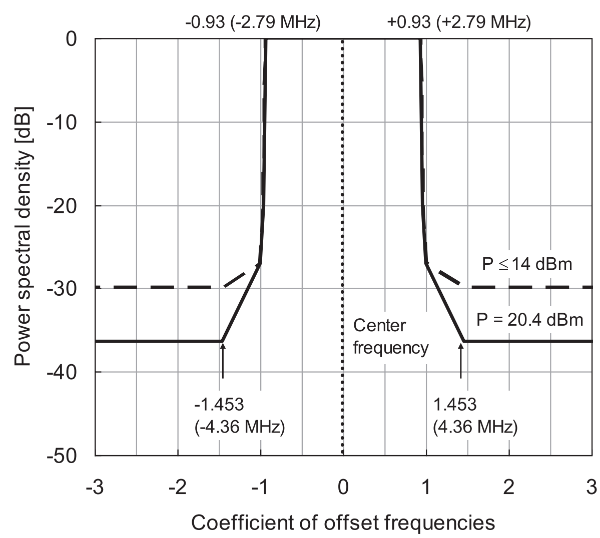

Fig. 13 Spectrum mask.

at another location. The configuration may also include a receiving antenna in place of a transceiver, such as in the case of a broadcast signal repeater. Considerations for the target system are listed below.

- RoF systems including the sub carrier multiplexing (SCM) systems that perform analog optical modulation of single-channel or multiple-channel signals.
- "Digital RoF" transmission systems, in which a high-frequency modulated signal is converted to a digital signal (analog to digital conversion) for transmission and the digital output of the OE is then converted to analog (digital to analog conversion) are outside the application of this specification.
- Link configuration: the optical networks part can have any configuration.

The spectrum mask and the unwanted emission are specified as the signal quality factors to be satisfied as hardware specifications. For the downlink transmission signal,

Table 4 Transmission spectrum break points.

Coefficients of offset frequencies from center frequency		Power spectral density [dB]	
DTTB system A, C, mobile communication	DTTB system B	$P_{sig}\leq 14$ dBm	14 dBm$<P_{sig}\leq 20.4$ dBm
±0.93	±0.952	0	
±0.953	±0.975	-20	
±1	±1	-27	
±1.453	±1.453	-30	$-16-P_{sig}$

DTTB system A: ATSC [17] (U.S.A.)
DTTB system B: DVB-T [18] (E.U.)
DTTB system C: ISDB-T [19] (Japan)

the break point specifications are listed in Table 3 and the spectrum mask is shown in Fig. 13. In the DTTB system A [17], B [18], and C [19] are defined in ITU-R Recommendation BT.1306-6 [20]. P_{sig} indicate an average signal power per channel. The equipment must satisfy the specifications at the terminal for connection to the antenna. For the purpose of dealing with the DTTB systems and mobile communication together, the offset frequencies from center frequency are represented by coefficients. To convert from the coefficients to frequencies, multiply by 3 MHz, 3.5 MHz, or 4 MHz for DTTB and multiply by 2.5 MHz for mobile communication. The frequencies in parentheses in Table 4 are frequencies applied to 6-MHz bandwidth DTTB systems A and C as one example.

In the case of determining the spectral mask, for multiple adjacent channel signals and the spectral mask is applied at the break point on the low frequency side of the lowest carrier wave and at the break point on the high frequency side of the highest carrier wave.

To prevent interference with other radio services, filters that suppress unwanted emission in the relevant frequency bands are recommended.

Equipment that radiates DTTB signals satisfy the specifications listed in Table 5. Devices that radiate downlink signals for mobile communication (base station to mobile terminal, etc.) shall satisfy the standard, ARIB STD-T63-25.A01 V8.0.0, Sect. 9.2 [21].

6. Conclusion

This paper described the outline of standardization activities for Radio on Fiber (RoF) transmitter of IEC TC103/WG5. The outline of the proposed standards such as measurement method of E/O devices, O/E devices and acceptable technical specification of RoF transmitter are described. The National Committee of TC103/WG5 proposed four new work items. One is a committee draft, the second a technical specification, and two others are new work item proposals. These documents are now drafted by TC103/WG5. The scope of RoF transmitter technology is expanding rapidly, according to the increase of number of wireless devices and systems. Furthermore, the standardization needs of RoF transmitter are more increasing. Therefore, the standard of TC103/WG5 is very important for future wireless communication devices, systems and infrastructures.

Table 5 Unwanted emission specification for DTTB.

Item	Specification
Spurious emission in the out-of-band domain	100 μW or less
Unwanted emission in the spurious domain	25 μW or less

NOTE
Spurious emission is an emission at a frequency or frequencies which are outside the necessary bandwidth and the level of which may be reduced without affecting the corresponding transmission of information. Spurious emissions include harmonic emissions, parasitic emissions, intermediation products, frequency conversion products, and single sideband phase noise, but exclude out-of-band emissions.
Out-of-band emission is an emission in a frequency or frequencies immediately outside the necessary bandwidth which results from the modulation process, but excluding spurious emission. The boundary between the out-of-band and spurious domain occurs at a separation of ±250 % of necessary bandwidth.

Acknowledgments

We would like to thank all the member of IEC TC103 and IEC TC103/WG5.

This project was funded by the Minister of Economy, Trade and Industry Japan for the international standardization work.

References

[1] A. Chen and E. Murphy, Broadband optical modulators: Science, Technology, and Applications, CRC Press, 2012.
[2] H. Ito, T. Furuta, F. Nakajima, K. Yoshino, and T. Ishibashi, "Photonic generation of continuous THz wave using uni-traveling-carrier photodiode," J. Lightwave Technol., vol.23, no.12, pp.4016–4021, Dec. 2005.
[3] T. Ishibashi, N. Shimizu, S. Kodama, H. Ito, T. Nagatsuma, and T. Furuta, "Uni-traveling-carrier photodiodes," Tech. Dig. Ultrafast Electron. and Optoelectron (1997 OSA Spring Topical Meeting), pp.166–168, 1997.
[4] ISO/IEC Directives, Part 1, "Procedures for the technical work," 9th ed., 2012.
[5] ISO/IEC Directives, Part 2, "Rules for the structure and drafting of international standards," ed. 6.0, 2011.
[6] IEC/PAS 62593/Ed.1, "Measurement method of a half-wavelength voltage for Mach-Zehnder optical modulators in wireless communication and broadcasting systems," 2008-11.
[7] IEC 62801 Ed. 1.0, "Measurement method of a half-wavelength voltage for mach-zehnder optical modulator in wireless communication and broadcasting systems," 2012-10. to be published.
[8] IEC 62800 Ed. 1.0, "Radio on fiber system conforming to different spectral emission standard," 2012-10. to be published.
[9] IEC 62802 Ed. 1.0, "Measurement method of a half-wavelength voltage and a chirp parameter for mach-zehnder optical modulator in high-frequency Radio on Fibre (RoF) systems," 2012-10. to be published.
[10] IEC 62803 Ed. 1.0, "Measurement method of frequency response of O/E conversion devices for high-frequency radio on fibre (RoF) systems," 2012-10. to be published.
[11] T. Kawanishi, K. Kogo, S. Oikawa, and M. Izutsu, "Direct measurement of chirp parameters of high-speed Mach-Zehnder-type optical

modulators," Opt. Commun. 195, pp.399–404, 2001.
[12] S. Oikawa, T. Kawanishi, and M. Izutsu, "Measurement of chirp parameters and halfwave voltages of Mach-Zehnder-type optical modulators by using a small signal operation," IEEE Photonics Technol. Lett., vol.15, no.5, May 2003.
[13] T. Kawanishi, "Parallel Mach-Zehnder modulators for quadrature amplitude modulation," IEICE Electronics Express, vol.8, no.20, pp.1678–1688, Oct. 2011.
[14] K. Inagaki, T. Kawanishi, and M. Izutsu, "Optoelectronic frequency response measurement of photodiodes by using high-extinction ratio optical modulator," IEICE Electronics Express, vol.9, no.4, pp.220–226, Feb. 2012.
[15] T. Kawanishi, T. Sakamoto, A. Chiba, M. Tsuchiya, and H. Toda, Ultra high extinciton-ratio and ultra low chirp optical intensity modulation for pure two-tone lightwave signal generation, CLEO2008, CFA1.
[16] K. Inagaki and T. Kawanishi, "Calibration method of optoelectronic frequency response using Mach-Zehnder modulator," Proc., IEEE MWP 2010, pp.143–146, 2010.
[17] ATSC: Advanced Television Systems Committee standards, http://www.atsc.org/cms/index.php
[18] DVB-T: Digital Video Broadcasting Terrestrial, http://www.dvb.org/index.xml
[19] ISDB-T: Integrated Services Digital Broadcasting Terrestrial, http://isdb-t.jp/en/index.html
[20] ITU-R BT.1306-6, "Error correction, data framing, modulation and emission methods for digital terrestrial television broadcasting," Dec. 2011.
[21] ARIB STD-T63-25.A01 V8.0.0, "The low power repeaters for DS-CDMA, section 9.2 spurious emissions," pp.13–17, Dec. 2009.

Satoru Kurokawa received the B.E. and M.E. degrees in electrical engineering from Chiba University, in 1987 and 1989, respectively, and the Ph.D. degree from Department of Communication and Computer Engineering, Kyoto University, in 2003. From 1989 to 2003, he was worked for Kyoto prefectural government. He has been working as a Section chief of Electromagnetic Field section with the Metrology Institute of Japan, National Institute of Advanced Industrial Science and Technology, Ibaraki, Japan, since 2003. He is currently working on antenna metrology and microwave and millimeter-wave photonics for antenna measurement.

Junichiro Ichikawa received his B.S. and M.S. degrees in mineralogy from the University of Tokyo in 1987 and 1989, respectively. He joined the Optoelectronics Division of Sumitomo Osaka Cement Co., Ltd. in 1989 and has been engaged in development of optical devices using dielectric materials. His recent research interests are in micro-fabrication process of ferroelectric materials for optoelectronics and electronics applications. He received the Sakurai Memorial Award from the Optoelectronic Industry and Technology Development Association (OITDA) of Japan in 2007 for the development on integrated lithium-niobate optical modulators.

Tetsuya Kawanishi received the B.E., M.E. and Ph.D. degrees in electronics from Kyoto University, in 1992, 1994 and 1997, respectively. From 1994 to 1995, he worked for Production Engineering Laboratory of Matsushita Electric Industrial (Panasonic) Co., Ltd. In 1997, he was with Venture Business Laboratory of Kyoto University, where he had been engaged in research on electromagnetic scattering and on near-field optics. He joined the Communications Research Laboratory, Ministry of Posts and Telecommunications (from April 1, 2004, National Institute of Information and Communications Technology), Koganei, Tokyo, in 1998. In 2004, he was a Visiting Scholar at the Department of Electrical & Computer Engineering, University of California at San Diego, USA. He is now a Director of Lightwave Devices Laboratory, Photonic Network Research Instiitute, National Institute of Information and Communications Technology, and is currently working on high-speed optical modulators and on RF-photonics.

Hiroyo Ogawa received the B.S., M.S., and Dr. Eng. degrees in electrical engineering from Hokkaido University, Sapporo, in 1974, 1976, and 1983, respectively. He joined the Yokosuka Electrical Communication Laboratories, Nippon Telegraph and Telephone Public Corporation (NTT), Japan, in 1976. Since then, he has been engaged in the research, development and standardization on microwave and millimeter-wave circuits and systems at NTT Wireless Systems Laboratories, ATR Optical and Radio Communication Research Laboratories, and Communication Research Laboratory, Ministry of Posts and Telecommunications, and New Generation Wireless Communications Research Center, National Institute of Information and Communications Technology (NICT). He is now a Vice Director General of Association of Radio Industries and Businesses (ARIB). He has contributed to make novel microwave and millimeter-wave integrated circuit technologies, optically-fed millimeter-wave access systems which are known as Radio-on-Fiber (RoF), and millimeter-wave short-range systems using 60-GHz unlicensed frequency whose standard are now discussed within IEEE802.15.3c. He also contributed MTT-S as an associate editor of MGWL, member of IMS TPC and a few MTT-S Technical Committees. He served several international conferences or meetings such as APMC (Asia-Pacific Microwave Conference), MWP (Topical Meeting on Microwave Photonics), AP-MWP (Asia-Pacific Microwave Photonics Conference), TSMMW (Topical Symposium on Millimeter Waves), and IEEE802.15.3c Task Group, as a chair or vice-chair of each committee. He also serves APT Standardization Program (ASTAP) as a chairman of MMCS (Millimeter-wave Communication Systems) Expert Group, and several Telecommunications Councils of Ministry of Internal Affair and Communications (MIC) as a member, and is now contributing several Working Parties of ITU-R (International Telecommunication Union — Radio Sector). He currently serves as a convener of IEC TC103 WG6 which standardizes Radio on Fiber (RoF) transmitter related technologies. He is a fellow of IEEE.